¹⁰Be at iThemba LABS using a silicon nitride membrane stack as absorber for isobar suppression

Authors

Winkler $S.^{1,2,*}$, Mbele $V.^{-1}$, Khosa $R.^{-1,3}$, Corbett $L.B.^{-4}$, Bierman $P.^{-4}$, Hidy $A.^{-5}$, Brown $T.^{-5}$, Makhubela $T.V.^{-3}$, Kramers $J.^{-3}$, Tooth $S.^{-6}$

Affiliations

- ¹ TAMS Department, iThemba LABS, Johannesburg, South Africa
- ² Accelerator mass spectrometry and isotope research, Helmholtz-Zentrum Dresden-Rossendorf, Germany
- ³ GRIT Centre, Department of Geology, University of Johannesburg, Johannesburg, South Africa
- ⁴ Rubenstein School of the Environment and Natural Resources, University of Vermont, Vermont, USA
- ⁵ Center for Accelerator Mass Spectrometry/Lawrence Livermore National Laboratory, California, USA
- ⁶ Department of Geography and Earth Sciences, Aberystwyth University, Aberystwyth, Wales, United Kingdom
- * Corresponding author, current affiliation: Accelerator mass spectrometry and isotope research, Helmholtz-Zentrum Dresden-Rossendorf, Germany

Abstract

¹⁰Be is an important isotope for accelerator mass spectrometry (AMS) because of the demand for cosmogenic radionuclide dating methods in the earth science and paleo-sciences community. At the iThemba Laboratory for Accelerator Based Science (iThemba LABS) we implemented full suppression of the interfering isobar ¹⁰B using a silicon nitride foil-stack, utilizing the 2+ charge state for high efficiency. We demonstrate the performance of this newly established AMS system using standards and test samples. We further present the results of an inter-comparison between iThemba LABS and the Center for Accelerator Mass Spectrometry/Lawrence Livermore National Laboratory, prepared as AMS sample from the purified quartz at University of Vermont. The results for ¹⁰Be from the laboratories are

in close agreement, fully consistent with cross-calibration between them. AMS results for ²⁶Al are in similarly good agreement, demonstrating the performance and accuracy of iThemba LABS for the most commonly measured in situ produced cosmogenic nuclides.

Keywords

10-Be; isobar separation; accelerator mass spectrometry;

1 Introduction

Accelerator mass spectrometry (AMS) is a technique used mostly to measure long-lived radioisotopes in the environment, most prominently amongst them ¹⁴C, ¹⁰Be, and ²⁶Al. These isotopes have a wide and increasing range of applications, e.g. in heritage studies, environmental science, ecology, and geology.[1-3] Although there are more than 100 such facilities world-wide [4], and despite rich opportunities for such studies all over Africa, the iThemba Laboratory for Accelerator Based Science (iThemba LABS) hosts the first, and currently only, AMS system on the African continent.

The AMS system of iThemba LABS is situated in Johannesburg, South Africa, on a sub-campus of the wider University of the Witwatersrand campus. The system was implemented in several stages starting in 2005 with the refurbishment of the 6 Megavolt linear tandem accelerator (HVEE EN Model), the construction of an ion-source and AMS injector beamline, with the final elements – a modern AMS analyzing beamline supplied by NEC – installed in 2014 [5]. The AMS system was opened in July 2014, after the installation of this high-energy side beamline.

The key to the superiority of AMS versus other mass spectrometry regarding the isotopic abundance limit of detection, is the isobar suppression capability. In the case of ¹⁴C and ²⁶Al, isobar suppression already is conveniently delivered by the negative ion formation process, which excludes extraction of the elemental ions of nitrogen and magnesium, respectively, although there is a requirement for isobar separation techniques (such as the gas-filled magnet for accelerators >5MV [6-8], and the newly established techniques based on laser-photo-detachment in an ion-cooler [9]) if one is to use AlO for injection. In any case, for ¹⁰Be the key problem is that the interfering isobar of ¹⁰B does form negative ions, and so does boron oxide, meaning that isobar separation has to be accomplished at some point after the ion source. Consequently, we have been quickly able to verify our system for ²⁶Al [10,11] and then – after some improvements of our AMS system – for ¹⁴C [12]. On the other hand for ¹⁰Be we still had work to do, because of the need for isobar suppression at the detector stage rather than in the ion source. Initially, there was an added obstacle of low achievable terminal voltages (3.5 MV or less), which made using the gas absorber cell an untenable approach. The gas absorber employs a separate gas cell filled with nitrogen before the detector to fully stop the interfering isobar ¹⁰B, while the lesser stopping power for ¹⁰Be leaves it with residual energy for a signal in the subsequent detector. Removing ¹⁰B before detection is important as the typical boron beams from the AMS samples would overwhelm

the count-rate capability of any particle detector. Significant energy is needed for the standard setup to work, using the 3+ charge state, which comes with an additional cost of low charge state transmission through the accelerator with iThemba LABS' accelerator actual capabilities.

Recent studies have shown that low-stress silicon nitride membranes can be used as absorber foil for full stopping of the interfering isobar ¹⁰B with a particle energy as low as 6 MeV for the measurement of ¹⁰Be [13]. We present here the implementation of this approach to full stopping of ¹⁰B in ¹⁰Be-AMS for our larger AMS system with a full assessment of the measurement capability for earth science applications, and present our own Be-carrier material (extracted from a phenakite crystal) that is superior to the commercially available materials typically used by other laboratories. In our final setup, we use a terminal voltage of 4.180 MV and the 2+ charge state, giving a ¹⁰Be²⁺ beam energy of 10.008 MeV going into the detector system.

We then present experimental evaluation of the impact of ¹⁰B current on the detection limit, using our low-level beryllium carrier material, and a dilution series of standards, from the set available from K. Nishizumi [14]. Furthermore, we demonstrate the proficiency of our approach in a laboratory intercomparison with the Center for Accelerator Mass Spectrometry at Lawrence Livermore National Laboratories (CAMS/LLNL), using 14 AMS field samples prepared from purified quartz at the University of Vermont (UVM). We also demonstrate here that our ²⁶Al analyses reproduce well those made at LLNL.

2 The iThemba LABS AMS system for $^{10}\mbox{Be}$

The iThemba LABS AMS system [5,11,15] is based on: (i) an in-house built Middleton type ion source similar to a design used at CAMS/LLNL [16]; (ii) an in-house constructed injector with an electrostatic analyser, analysing magnet, and a bouncing chamber for fast-sequencing; (iii) a pelletron-refurbished 6 MV EN tandem; and (iv) a high-energy beamline supplied by National Electrostatics Corporation (NEC), Wisconsin, as is typically found at 5 MV tandems [17], with minor modifications. A schematic drawing showing the sequence of the major AMS components discussed in the further is shown in Figure 1.

The ion source has an automated mechanical sample changing mechanism, which inserts and extracts front loaded sample holders to the measurement position from a wheel that can contain up to 64 sample holders. We ran the extraction at 40 kV (in principle up to 70 keV injection voltage is possible), the ionizer at 130-135 W, and the cathode voltage at 8.5 kV at the time of the experiments presented here, as limited by arcing in the ion source. X and Y steerers and two Einzel lenses are placed after the extraction.

The low-energy mass spectrometer comprises a 90° cylindrical electrostatic analyzer with a radius of 306 mm and a gap of 50 mm, and a 90° analyzing magnet with a radius of 608 mm and a pole gap of

94 mm. The magnet chamber is insulated and its potential can be driven with a power amplifier to allow fast sequencing. Currently, the theoretical voltage range we have available is +/-5 kV, but due to an insertable lense, required for the ion beam analysis capabilities established prior to AMS [18,19], the magnet chamber's gaps could not be placed in their ideal positions, resulting in a differential in focusing for different mass settings of the bouncing system. Consequently, we use only a range from 0 to -5 kV (14C) or 0 to +5 kV (for ¹⁰Be and ²⁶Al). At 40 kV, this range is sufficient for 13 amu versus 14 amu bouncing (as in radiocarbon AMS), with enough overlap in the focusing between the isotopes if the tuning is good. For ¹⁰Be measurements, the situation is even easier as we are injecting a mass of 25 amu (9Be¹⁶O) versus 26 amu (¹⁰Be¹⁶O). The low-energy side offset cup is fixed in position at mass 13, a change from the original setup and improvement with regards to focusing relative to the off-set cup longitudinal position. In addition, this setup allows for both mass 12 and 13 low-energy side monitoring during cycling, as the offset cup can cover both mass 13 when injecting 14, and mass 12 when injecting 13. After the magnet chamber, we have two Einzel lenses, one X and one Y steerer, and an additional set of fast-switching X and Y steerers as part of the bouncer setup, ensuring beam transport through the gas stripper for both the reference and the rare isotope. For ¹⁰Be AMS we set our injection magnet to transmit mass 25 at a bouncer voltage of 4.5 kV, which results in transmission of 26 at approximately 2.8 kV. Keeping these voltages as similar as possible mitigates the differential in focusing, and there is no problem with transmission through the accelerator when using positive as opposed to negative voltages. An additional cycle at 1.3 kV allows to monitor BeO on the low energy side.

The accelerator features a Q-snout lens at the entrance, and has a recirculating gas stripper with a tube diameter of 9.2 mm. We use argon as stripper gas. The insulating gas for the accelerator tank is a mixture of N₂ (80%) and CO₂ (20%) and there is clear evidence of insulation gas leakage into the gas stripper system, as discerned from ¹⁴C measurements. The ¹⁴N ions from the gas stripper get charged and recharged to 3+, with some of them picking up the right energy to match ¹⁴C³⁺, and show up as background in the detector. Even at 18 bar of pressure, high terminal voltages could not be achieved. Consequently, the pressure was reduced to 13 bar to reduce this leakage to an acceptable level, thereby improving both the background and the stability of the machine.

The stripper background of ionized gas atoms, however, should not directly affect ¹⁰Be, since the m/q interference of ¹⁵N³⁺ even with the appropriate energy to pass the analyzing beamline, would be stopped by an absorber the same as the interfering isobar ¹⁰B²⁺. More problematic for ¹⁰Be is that the stripper gas density originally was not well controlled at high settings of our leak valve. Since we do not have any direct pressure measurement in our re-circulating stripper, we have to rely on the vacuum readings at the high-energy and low-energy base of the accelerator, and the charge state transmission, which is a function of stripper gas pressure. We have replaced our original setup of a thermo-mechanical leak valve with a needle valve operated with a precision stepper motor, with the desired effect of better stability of the stripper gas pressure over time.

Post accelerator, the first 90° magnet is for the ion beam analysis and nuclear physics beamlines and consequently is de-gaussed for AMS. An electrostatic triplet and two steerers in X and Y each are available to transport the beam through the 0° port of this magnet. The NEC high-energy side beamline for AMS is placed after this magnet. The start of the analyzing beam line features an electrostatic duplet to refocus the beam to the image point of the magnet, and an electrostatic Y-steerer (at present the last Y-steerer). The analyzing magnet is a 90°, double-focusing one, and has a radius of 1270 mm and a pole gap of 34 mm. After the analyzing magnet, the following sequence is found: the chamber for the movable offset cups (two inside for 9Be, 12C, and 13C – one outside used for 27Al), a magnetic quadrupole duplet, a 20 degree cylindrical electrostatic analyzer, a switching magnet, and the detector beamline featuring another magnetic quadrupole duplet, and a gas ionization chamber.

3 Detector system and ¹⁰B suppression

The multi-anode gas ionization chamber is the NEC version described by Maden, et al. [17] We use the first employ the first two Anodes as described there, however, the rest of the sections have been connected together to provide only one further Anode. We use the latter only for ²⁶Al and ¹⁴C measurements. Detector signals from the ionization chamber are amplified by CoolFET pre-amplifier (AMPTek A250CF), then the ORTEC 570 spectroscopy amplifier. The amplifier output is digitized using a PIXIE module, which is part of the NEC delivered data acquisition system. This allows us to obtain files of time-stamped (or rather cycle-stamped) single event raw data concurrently with a cycle-by-cycle record of the reference currents, when operated using NEC's data acquisition software DMAN [17].

Usually, this detector is operated in a configuration that electrically connects the detector entrance window (100 nm silicon nitride, 8x8 mm, by Silson, Ltd., UK) and its holder to the cathode of the gas ionization chamber. In view of the pico-Ampere currents of ¹⁰B stopping in the foil-stack and the potential for signal to be transferred to the cathode, however, we insulated the window holder for ¹⁰Be against the cathode in order to leave it to "float" and not affect our cathode (total energy) signal. So far, we have not seen any time-dependent effect on the signals.

We have adopted isobutane (R600a) as our detector gas, using a pressure of $2.3 \cdot 10^3$ Pa. The cathode is biased at -135 V, the anodes at 225 V, and the grid at half of the anode voltage. In general, for 10 Be we can expect less lateral straggling due to avoiding a heavy nucleus like argon. Isobutane also allows for lower gas pressures at constant stopping range than other choices (e.g. propane, P10), which is easier on the thin silicon nitride detector windows.

A common recent approach has been the use of a low-stress silicon nitride degrader foil in combination with a high resolution electrostatic analyzer [20]. Such arrangements can perform extremely well at 3-5 MV using the 2+ charge state at the analyzing magnet, and at 3+ or 4+ charge state, after the degrader foil with background levels for 10 Be/ 9 Be of $\sim 5 \cdot 10^{-16}$ within the possibilities, however high precision

seems to require high particle energy and an analyzing beamline designed for this purpose [13,20]. It is also used widely in low-energy AMS setups [21,22]. The use of the 2+ charge state provides a large improvement in efficiency over the 3+ charge state at these terminal voltages, but some of that improvement is lost due to the degrader foil charge state distribution at terminal voltages below 5MV [23]. For us, the implementation of a degrader foil was not an option, as we lacked the high-resolution electrostatic analyzer setup. We would also have to rework the beamline to accommodate the degrader.

Low-stress silicon nitride seems to have been effective as a passive absorber in many instances, so it may look surprising that only recently has one AMS laboratory taken the step of trying a setup of full-stopping with a silicon nitride foil stack [13]. This setup at VERA (University of Vienna) has performed well in measurements with regards to background, corresponding to a ¹⁰Be/⁹Be-ratio of few times 10⁻¹⁶. As a feasibility experiment, this method was even tried at the Centre for Nuclear and Accelerator Technologies (CENTA), Bratislava, a facility which at that stage entirely lacked a high-energy analyzing beamline. The achieved background-ratio of (10⁻¹²), which – while insufficient for typical ¹⁰Be measurements – is still remarkable [24]. It has since also been tested at lower energies at the SARA facility (Centro Nacional de Aceleradores, Seville, Spain). [25]

We implemented our foil stack as two protruding threaded rods on the detector window holder (for photo see supplementary Figure 1), which can accommodate holders for the silicon nitride membranes in front of the detector's silicon nitride window with 100 nm thickness, 8x8 mm window size, and 14x14 mm frame. Our silicon nitride membranes for the foil-stack are 1000 nm in thickness, sized 8x8 mm, with a frame dimension of 14x14 mm. These were glued onto duro aluminum frames, which were then slid onto the rods. The frames space the membranes 1.5 mm apart. The exact combination of the total foil thickness and energy was determined experimentally.

Our AMS samples for ¹⁰Be measurements are in BeO form mixed with niobium ~1:4 by weight. For our initial tests, we had the set of ¹⁰Be AMS standards by K. Nishiizumi [14], already in oxide form, and a bottle of high purity BeO (Sigma Aldrich) as a test blank.

4 Setting the foil-stack thickness

In setting up the foil thickness, there are three main considerations: (i) achieving the highest efficiency for $^{10}\text{Be}^{2+}$ by minimizing loss through angular straggling; (ii) keeping low the impact of the nuclear reaction on background and background level consistency, which favors lower particle energies; (iii) and getting a high residual energy of ^{10}Be , which favors higher particle energy, for good signal-to-noise ratio and thus better capacity to deal with any backgrounds in the detector.

In the first instance, we aimed for the highest energy obtainable, to keep transmission high and to get a high residual energy for maximum signal-to-noise ratio. The downside is potentially increased impact of the nuclear reaction background. This compromise was necessary because our detector resolution, as

discerned from ¹⁴C of 14 MeV incident energy, has only been around 0.8 MeV – full-width at half maximum.

To arrive at optimum thickness, we took residual energy spectra of ¹⁰B at nominal foil stack thicknesses of 1000, 3000, 6000 and 7000 nm for a terminal voltage of 4.006 MV, cross-calibrating when the amplifier settings needed changing. We then simulated the stopping (using SRIM [26]) of ¹⁰B in silicon nitride keeping the nominal thickness fixed, but using the density as free parameter to match the experimental results. A good match requires an effective density of 2.9 g/cm³. We then used this effective density to simulate the stopping of ¹⁰B and ¹⁰Be for the 9000 nm foil stack. This final simulation suggested that we could go up to 4.200 MV for this thickness and expect a residual signal for ¹⁰Be of 1.6 MV, while stopping ¹⁰B fully before the detector window. Spectra and simulations for boron are shown in Figure 2. The effective density inferred is on the low side of literature values for low-stress silicon nitride membranes, but still agrees reasonably (e.g. [27]). One possibility is that the stopping power for ¹⁰B over this energy range is higher than the SRIM model suggests, or else the actual thickness of the membranes is higher than quoted.

5 Detector signals and particle identification

In using the 2+ charge state, ${}^{9}BeH^{2+}$ needs to be given real consideration, as this molecular ion is stable, and consequently represents potential background for ${}^{10}Be$ in the detector [28]. At stripper gas settings as low as is used for ${}^{14}C$ measurements (for which we use the 3+ charge state at the high energy side), this background completely overwhelms our detector. To eliminate this background, sufficient collisions in the stripper are needed. As the stripper gas pressure increases, the count rate for ${}^{9}BeH^{2+}$ becomes manageable [28]. The species identifiable in the sample spectrum shown in Figure 3 are ${}^{10}Be$, ${}^{9}BeH$, and ${}^{9}Be$ from ${}^{9}BeH$ break-up with loss of the H before the detector's active volume. The expected mean energies based on SRIM for these are 1.6 MeV, 1.1 MeV, and 0.7 MeV, respectively. The ${}^{9}BeH$ is clearly separated in the cathode signal (E_{tot}) and does not present a fundamental problem unless its count rate moves above 1000 counts/s. Despite this, there are other reasons to keep ${}^{9}BeH$ fully suppressed, as is discussed below.

As stated before, in 10 Be measurements our detector is set to a pressure of $2.3 \cdot 10^3$ Pa. For this pressure full stopping is expected for 10 Be in the first anode. The current achievable resolution for our detector is insufficient to try for a 2^{nd} anode signal. Obviously, in our case the Anode (" Δ E1") does not contribute to separation of 9 BeH in any significant way but the 2D spectrum is useful as it removes some both noise events from the 10 Be bin that would be present in the E_{tot} spectrum, but also remove some types of background, while reducing others.

Suppression of 9 BeH to a level that allows for measurement requires quite high stripper gas pressure: In normal 14 C operating conditions, we would have a vacuum reading at the base of the accelerator of $5 \cdot 10^{-5}$ Pa, and at these levels we are also optimum for maximum transmission of 9 Be. However, the

detector would be completely overwhelmed with ${}^{9}BeH$ events, with count rates exceeding 10000 counts/s. We need to operate with a base vacuum of $\sim 1.5 \cdot 10^{-4}$ Pa to suppress the ${}^{9}BeH$ reliably. This is not a convenient value to operate, since we start experiencing occasional voltage breakdowns at base vacuum readings of $3 \cdot 10^{-4}$ Pa. At iThemba LABS we have only the vacuum at the base of the accelerator and transmission as indicator of stripper gas pressure, as there is currently no measuring gauge implemented in the gas stripper.

One of the problems with using base vacuum as an indicator is that we see significant delays in the response. Keeping track of the transmission – defined as high-energy mass 9 divided by low-energy mass 25 particle current – has proven to be a more reliable indicator. At low stripper gas settings, the charge state transmission for 2+ can be maximized to ~45% for our standard ¹⁰Be operational terminal voltage of 4.180 MV. When increasing the stripper gas pressure so that transmission drops below 35%, ⁹BeH²⁺ is sufficiently suppressed to make ¹⁰Be identification possible. Increasing the stripper gas pressure even further (putting transmission below ~25%) means that background is completely and reliably eliminated, leaving only ⁷Be and ⁴He from the reaction of incident ¹⁰B on hydrogen in the absorber, the absorber hydrogen recoils of incident ions, and the legitimate ¹⁰Be events in the spectra. This is the gas stripper setting where we operate the actual measurements. For gas stripper settings corresponding to 20-27% the optimal setting of the high-energy spectrometer varies only marginally, with centering adjustment of the terminal voltage within 1‰ of the operational voltage. During this set of experiments we used both blanks and standard samples, using the standard sample's ¹⁰Be count rate to retune to optimum transmission through the high-energy mass spectrometer.

The background of hydrogen recoils from incident ^{10}B in the absorber has been discussed by Lachner, et al.[29], and Scognamiglio, et al. [25], however for ^{10}Be -AMS at lower energies. For our specific setup a similar investigation using SRIM shows that the maximum signal for hydrogen recoils picked up by the cathode is expected below 0.8 MeV, less than half of the expected ^{10}Be signal of 1.6 MeV, while the corresponding ΔE_1 signal (the first Anode being 68 mm long) is expected to be below 0.3 MeV. In the 9BeH -free spectra for the blank-tests given in Figure 5 we can clearly identify a low-energy peak roundly matching these parameters, although there may be an indication that the ^{10}Be is not yet fully maximized and higher terminal voltages may be attempted. Under typical measurement conditions present from prepared samples this background can be separated even with our current detector resolution. However, the wider background from the $^{10}B(p,\alpha)$, which can deposit more Energy than the hydrogen recoils, would need improvements in the detector resolution for further suppression.

6 Measurement of standard and blank materials

We tested the reproducibility, background, and operational limitations of our current setup in a number of measurement runs. A significant problem with our first test measurements was the stability of the stripper gas pressure, which varied considerably; the thermo-mechanical leak valve needed constant re-

adjustment to keep supply enough stripper gas for BeH suppression and yet with low enough pressure to prevent voltage breakdown due to tube arcs. In those first measurement runs, the charge state transmission in the acceptable range varied from 20-27%, leading to decreased reproducibility. Even with these problems, we could reproduce a dilution series of standard materials [14] with commercial BeO (Alfa Aesar) serving as a first blank.Results are shown in Table 1. Later on, with the modified gas stripper, transmission did not vary more than 1% over an hour, and generally we reproduced standard samples at or close to counting statistics (<1%) under these conditions.

7 Laboratory inter-comparison of 14 prepared quartz samples from South Africa

In one of our first geomorphology projects in South Africa, a total of 14 samples of quartzite and granite were collected from outcrops along Vaal river near Parys, Free State, to determine exposure history. The samples were pretreated at iThemba LABS using the methods of Kohl and Nishiizumi [30] to yield purified quartz, as confirmed by inductively coupled plasma optical emission spectrometry (ICP-OES) at the Spectrum Analytical Facility, University of Johannesburg. In the case of the granite samples also a step of froth floatation was included to efficiently remove mica before the etching. Beryllium and aluminum were isolated and purified at the National Science Foundation/University of Vermont (UVM) Community Cosmogenic Facility using standard methods [31]. The samples were prepared in two separate batches, each of which included a blank and a quality control sample [32]. The dissolved quartz samples were spiked with ~0.5 mg of Be carrier, about twice the usual mass, so that the final samples could be split for replicate analyses. Where needed, sufficient ²⁷Al was added so that the final purified Al fraction could be measured at both iThemba LABS and CAMS/LLNL.

The duplicate samples were analyzed for 10 Be/ 9 Be and 26 Al/ 27 Al at both iThemba LABS and CAMS/LLNL. CAMS/LLNL is well established and known for its capability in measuring 10 Be [33]. At both AMS facilities, samples were normalized to primary standard 07KNSTD3110 [14] for 10 Be and KNSTD30960 for 26 Al [34]. In the iThemba LABS measurement, AMS performance was stable, with output currents in the range of 2 to 2.5 μA of 9 Be $^{2+}$ (corresponding to 4-5 μA of BeO $^{-}$) across all samples and procedural blanks. The raw ratios for the 10 Be standard (nominal 2.851·10 $^{-12}$) were \sim 1.0·10 $^{-12}$, which includes a sizeable cut – removing \sim 50% of legitimate 10 Be events – to optimize background suppression versus 10 Be. Unlike the CAMS/LLNL setup, which uses a gas absorber cell, we cannot monitor boron currents continuously in the iThemba LABS measurement. Nevertheless, the 10 B current was checked for the samples after the first turn on all samples using a pico-amperemeter, and yielded a range of 10-20 pA over the samples. For comparison, the standards show 5-10 pA. At these low currents, the precision of our Faraday cup and amplifier is limited; even when averaging 32 readings, the mean will fluctuate 2-5 pA. Considering these limitations, we see a good homogeneity and performance in boron-suppression by the sample preparation chemistry. Based on the stable performance between

different samples, we can assume the background ratios of the chemistry procedural blanks to be representative in both ¹⁰Be and ¹⁰B based background, and then use these values to assess the combination of chemistry and machine background, subtracting accordingly.

Our results demonstrate a strong correlation between samples analyzed at iThemba LABS and CAMS/LLNL (Figure 4) for both ¹⁰Be and ²⁶Al. The fitted linear of the compared ¹⁰Be atoms per gram of sample has a slope of 1.010±0.018 and an offset of (0.5±3.1)·10⁻¹³, well within error consistent with a 1:1 line. The Pearson's r of 0.9993 for the fit shows the agreement of the data between the laboratories. The mean difference between the laboratories' results for individual samples is 1.7%. Mean uncertainties are 1.3% (CAMS/LLNL) and 2.0% (iThemba LABS).

The agreement for 26 Al is similarly good. The fitted linear has a slope of 0.988±0.027, and the offset of $(0.1\pm1.1)\cdot10^{-13}$ is not distinct from 0. The corresponding Pearson's correlation coefficient is 0.9993, same as for 10 Be. The mean difference between the datasets is just 2.2%, with the typical uncertainties given by both laboratories at 2%.

8 Achievable background level and background correction

From the experience with the prepared samples, our background control clearly is not optimal, and we relied heavily on the good quality of the sample preparation. Without low and reproducible boron content and 10 Be count rates far higher than background counts from the 10 B(p, α) 7 Be reaction on hydrogen targets in the absorber, a reliable result would not have been possible. One problem is that with the current detector resolution, we get a significant overlap between the 10 Be events and the 7 Be/ α with sufficient residual energy. Currently, we do not have enough signal relative to resolution for a proper Δ E/E identification. In the spectra, a significant amount of the reaction-induced background is outside the 10 Be bin (Figure 5). With a suitable blank material as carrier and a boron dilution series, it should be possible to verify and establish a background correction within the spectra, based on the background counts outside the 10 Be peak.

For this experiment we used a carrier material extracted from phenakite, which had been harvested from a mine at Klein Spitzkoppe, Namibia. [35] The available phenakite crystal had a mass of 1.184 g, yielding carrier for about 100 samples. Based on previous studies by Merchel et al. [36], this material should give a lower background ratio than a commercially sourced BeO. We then created a ¹⁰B-dilution series based on the carrier, with a series of additions of 0 µg, 40 µg, 120 µg and 360 µg of B (from a multi-element ICP-MS standard) per AMS sample. Sample spectra for the dilution series demonstrate the concept of boron-dependent background (Figure 5), and the impact of using a spectra-based background subtraction as opposed to a boron-current based one (which is not available in our approach). The background subtraction is based on determining the counts in the background bin for the hydrogen recoils (lower left bin in the spectra in Figure 5) versus the counts in the rare isotope bin. Although no recoil background is expected in the rare isotope been, but rather the background of ⁷Be and 4 He from the 10 B(p, α) reaction, both these background sources are proportional to the incident 10 B. Therefore, they should be at a fixed ratio over the duration of the measurement, as we do not expect material changes in the hydrogen available in silicon nitride over the course of a beam-time. Since the carrier has a demonstrated low level of ¹⁰Be, and the boron incidence and nuclear reaction background for the 360 µg sample is two orders of magnitude higher, the hydrogen recoil background bin events to Be-bin nuclear reaction events is established. The 120 μg and the 40 μg results clearly demonstrate the linear dependency of these two types of events and the validity of the correction, as shown in Figure 6. Further, Figure 6 demonstrates that the measured level of ${}^{10}\text{Be}/{}^{9}\text{Be}$ (8±3·10⁻¹⁶) is consistent with the expected nuclear reaction background, pointing to a possibly much lower actual ¹⁰Be content in the carrier. Nevertheless, the uncertainty of the correction and the measurement does have an impact, so at this stage we can only claim an upper limit of $\sim 1 \cdot 10^{-15}$.

Obviously, using this approach to background correction will require a boron-dilution sample with every AMS run for reference to remove the systematic problem and allow us to verify the actual detection limit for each prepared sample individually. This is important, as the limit may vary depending on the ¹⁰B incidence, which can be specific to each sample. Another advantage of the method is that we can use a wider bin for counting ¹⁰Be. Typical raw ratios for 07KNSTD3110 were 2.0·10⁻¹². We have applied this procedure to our most recent measurements [37].

9 Conclusions

We implemented a silicon nitride membrane absorber as the method to measure ¹⁰Be at the iThemba LABS AMS facility. We then successfully tested this setup using standard materials and blanks, and demonstrated linearity. The setup allows us to measure with good atom counting efficiency, although given the shortcomings of our gas ionization detector, the detection limit is degraded when the boron content of the AMS sample is high. Nevertheless, with good sample preparation, the inter-comparison with CAMS/LLNL demonstrated the capability of the iThemba LABS AMS system for ¹⁰Be. We then developed a way to control for boron-induced background from our spectra, using controlled boron-spiked samples and a Be-blank material as carrier. In this investigation, we could confirm this carrier ¹⁰Be/⁹Be to be at 1·10-¹⁵ or lower, and established this limit as our current detection limit under good measurement conditions. Further improvement will require an overhaul of the detector system, which can be implemented in the future. However, the current system is already performing well enough with several ¹⁰Be-projects completed or underway.

Acknowledgements

Stephan Winkler and Tebogo Makhubela would like to thank Stephan Woodborne for the Phenakite material used, and University of Witwatersrand for use of the WIGLabs metal free clean laboratory facility. Several grants have contributed to the funding: Field sampling was funded by Aberystwyth University. Work was supported by the National Research Foundation of South Africa, GRANT 98920 to Vela Mbele and AOGR 98837 to Stephan Winkler. Work done under support from NSF EAR-1735676 to Paul Bierman. Prepared in part by LLNL under Contract DE-AC52-07NA27344.

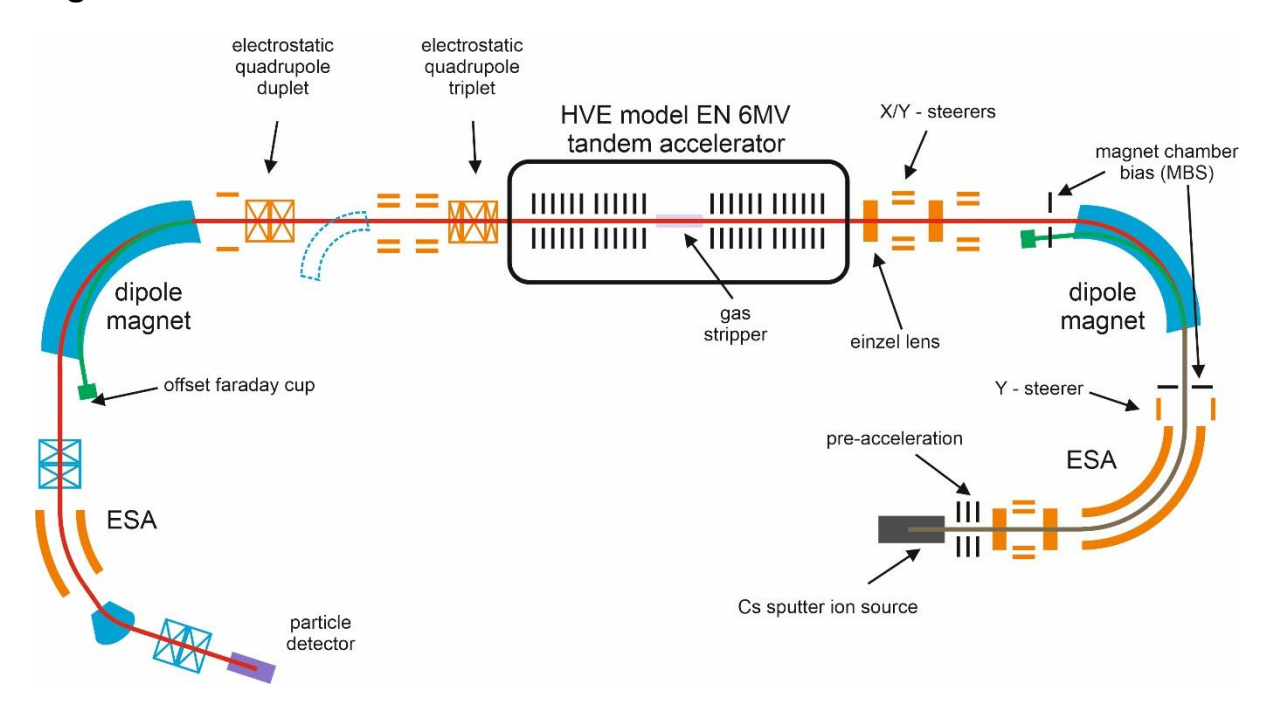
References

- [1] Muzikar, P., Elmore, D., & Granger, D. E. (2003). Accelerator mass spectrometry in geologic research. *Geological Society of America Bulletin*, 115(6), 643-654.
- [2] Fifield, L. K. (1999). Accelerator mass spectrometry and its applications. *Reports on Progress in Physics*, 62(8), 1223.
- [3] Kutschera, W. (2013). Applications of accelerator mass spectrometry. *International Journal of Mass Spectrometry*, 349, 203-218.
- [4] Kutschera, W. (2016). Accelerator mass spectrometry: state of the art and perspectives. *Advances in Physics: X*, *I*(4), 570-595.
- [5] Mbele, V. L., Mullins, S. M., Winkler, S. R., & Woodborne, S. (2017). Acceptance tests for AMS radiocarbon measurements at iThemba LABS, Gauteng, South Africa. *Physics Procedia*, 90, 10-16.

- [6] Fifield, L. K., Tims, S. G., Gladkis, L. G., & Morton, C. R. (2007). 26Al measurements with 10Be counting statistics. *Nuclear Instruments and Methods in Physics Research Section B: Beam Interactions with Materials and Atoms*, 259(1), 178-183.
- [7] Miltenberger, K. U., Müller, A. M., Suter, M., Synal, H. A., & Vockenhuber, C. (2017). Accelerator mass spectrometry of 26Al at 6 MV using AlO- ions and a gas-filled magnet. *Nuclear Instruments and Methods in Physics Research Section B: Beam Interactions with Materials and Atoms*, 406, 272-277.
- [8] Altenkirch, R., Feuerstein, C., Schiffer, M., Hackenberg, G., Heinze, S., Mueller-Gatermann, C., & Dewald, A. (2019). Operating the 120° Dipol-Magnet at the CologneAMS in a gas-filled mode. *Nuclear Instruments and Methods in Physics Research Section B: Beam Interactions with Materials and Atoms*, 438, 184-188.
- [9] Lachner, J., Martschini, M., Kalb, A., Kern, M., Marchhart, O., Plasser, F., ... & Golser, R. (2021). Highly sensitive 26Al measurements by Ion-Laser-InterAction Mass Spectrometry. *International Journal of Mass Spectrometry*, 465, 116576.
- [10] Makhubela, T. V., Kramers, J. D., Scherler, D., Wittmann, H., Dirks, P. H. G. M., & Winkler, S. R. (2019). Effects of long soil surface residence times on apparent cosmogenic nuclide denudation rates and burial ages in the Cradle of Humankind, South Africa. *Earth Surface Processes and Landforms*, 44(15), 2968-2981.
- [11] Makhubela, T. V., Winkler, S. R., Mbele, V., Kramers, J. D., Khosa, R. R., Moabi, H. P., & Konyana, S. M. (2021). Development of cosmogenic nuclide capabilities in South Africa and applications in Southern African geomorphology. *South African Geographical Journal*, *103*(1), 99-118.
- [12] Fisher, E. C., et al. (2020). Coastal occupation and foraging during the last glacial maximum and early Holocene at Waterfall Bluff, eastern Pondoland, South Africa. *Quaternary Research*, 97, 1-41.
- [13] Steier, P., et al. (2019). Comparison of methods for the detection of 10Be with AMS and a new approach based on a silicon nitride foil stack. *International Journal of Mass Spectrometry*, 444, 116175.
- [14] Nishiizumi, K., Imamura, M., Caffee, M. W., Southon, J. R., Finkel, R. C., & McAninch, J. (2007). Absolute calibration of 10Be AMS standards. *Nuclear Instruments and Methods in Physics Research Section B: Beam Interactions with Materials and Atoms*, 258(2), 403-413.
- [15] Sekonya, K. G. (2017). Development of 6 MV Tandem Acclerator Mass Spectrometry Facility and Its Applications (Doctoral dissertation, University of the Witwatersrand, Faculty of Science, School of Physics).
- [16] Southon, J., & Roberts, M. (2000). Ten years of sourcery at CAMS/LLNL-Evolution of a Cs ion source. *Nuclear Instruments and Methods in Physics Research Section B: Beam Interactions with Materials and Atoms*, 172(1-4), 257-261.
- [17] Maden, C., et al. (2007). SUERC AMS ion detection. *Nuclear Instruments and Methods in Physics Research Section B: Beam Interactions with Materials and Atoms*, 259(1), 131-139.
- [18] Msimanga, M., Wamwangi, D., Comrie, C.M., Pineda-Vargas, C.A., Nkosi, M., & Hlatshwayo, T. (2013). The new Heavy Ion ERDA set up at iThemba LABS Gauteng: Multilayer thin film depth profiling using direct calculation and Monte Carlo simulation codes. *Nuclear Instruments and Methods in Physics Research Section B:*Beam Interactions with Materials and Atoms, 296, 54-60.

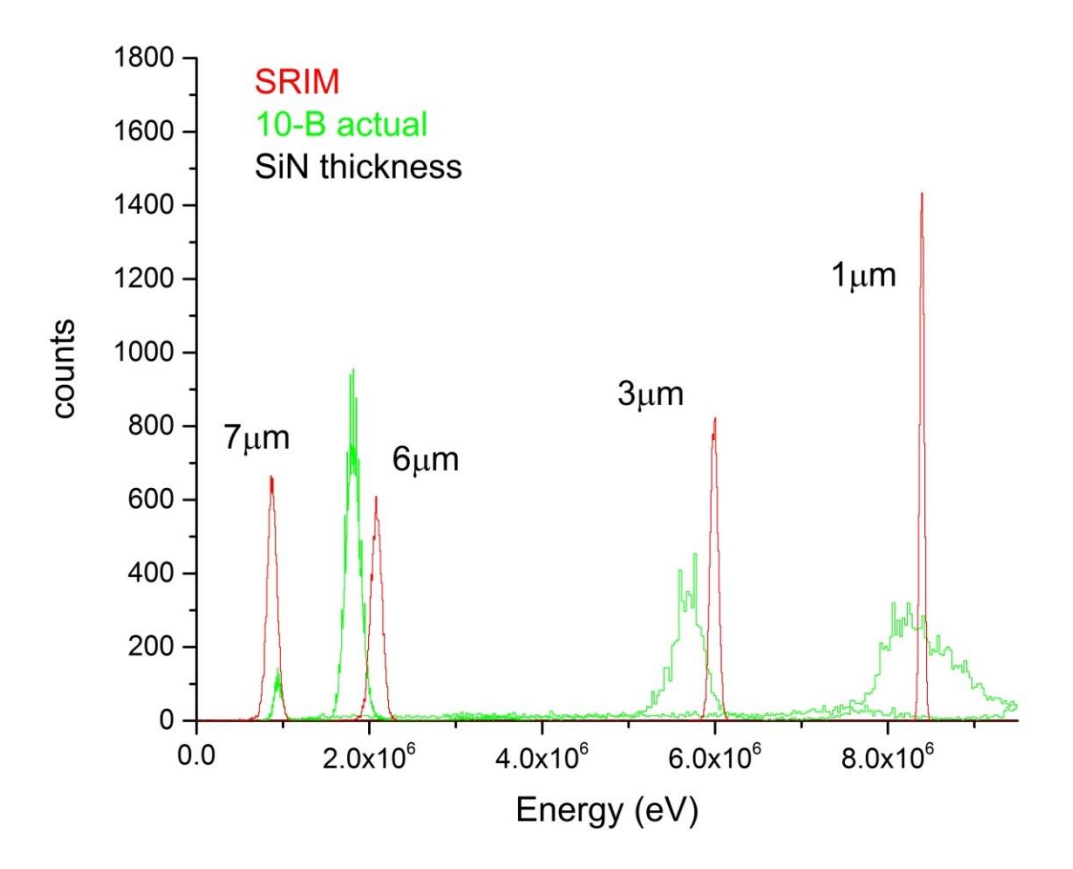
- [19] Buthelezi, K. V. (2008). Design of a negative helium ion injection system for the 6MV EN Tandem Accelerator at iThemba Laboratory for Accelerator Based Sciences. Master's Thesis, North-West University, South Africa.
- [20] Klein, M. G., et al. (2008). Performance of the HVE 5 MV AMS system at CEREGE using an absorber foil for isobar suppression. *Nuclear Instruments and Methods in Physics Research Section B: Beam Interactions with Materials and Atoms*, 266(8), 1828-1832.
- [21] Müller, A. M., Christl, M., Lachner, J., Suter, M., & Synal, H. A. (2010). Competitive 10Be measurements below 1 MeV with the upgraded ETH–TANDY AMS facility. *Nuclear Instruments and Methods in Physics Research Section B: Beam Interactions with Materials and Atoms*, 268(17-18), 2801-2807.
- [22] Heinemeier, J., Olsen, J., Klein, M., & Mous, D. (2015). The new extended HVE 1 MV multi-element AMS system for low background installed at the Aarhus AMS Dating Centre. *Nuclear Instruments and Methods in Physics Research Section B: Beam Interactions with Materials and Atoms*, 361, 143-148.
- [23] Lachner, J., Rugel, G., Vilches, C. V., Koll, D., Stübner, K., Winkler, S., & Wallner, A. (2023). Optimization of 10Be measurements at the 6 MV AMS facility DREAMS. *Nuclear Instruments and Methods in Physics Research Section B: Beam Interactions with Materials and Atoms*, 535, 29-33.
- [24] Ješkovský, M., Steier, P., Priller, A., Breier, R., Povinec, P. P., & Golser, R. (2015). Preliminary AMS measurements of 10Be at the CENTA facility. *Nuclear Instruments and Methods in Physics Research Section B: Beam Interactions with Materials and Atoms*, *361*, 139-142.
- [25] Scognamiglio, G., Lachner, J., Chamizo, E., López-Gutiérrez, J. M., & Priller, A. (2019). 10Be low-energy AMS with the passive absorber technique. *Nuclear Instruments and Methods in Physics Research Section B: Beam Interactions with Materials and Atoms*, 438, 113-118.
- [26] Ziegler, J. F., Ziegler, M. D., & Biersack, J. P. (2010). SRIM—The stopping and range of ions in matter (2010). *Nuclear Instruments and Methods in Physics Research Section B: Beam Interactions with Materials and Atoms*, 268(11-12), 1818-1823.
- [27] Mastrangelo, C. H., Tai, Y. C., & Muller, R. S. (1990). Thermophysical properties of low-residual stress, silicon-rich, LPCVD silicon nitride films. *Sensors and Actuators A: Physical*, 23(1-3), 856-860.
- [28] Wacker, L., Grajcar, M., Ivy-Ochs, S., Kubik, P., & Suter, M. (2004). 10Be Analyses with a Compact AMS Facility—Are BeF₂ Samples the Solution? Radiocarbon, 46(1), 83-88. doi:10.1017/S0033822200039382
- [29] Lachner, J., Christl, M., Müller, A. M., Suter, M., & Synal, H. A. (2014). 10Be and 26Al low-energy AMS using He-stripping and background suppression via an absorber. *Nuclear Instruments and Methods in Physics Research Section B: Beam Interactions with Materials and Atoms*, 331, 209-214.
- [30] Kohl, C.P., Nishiizumi, K., 1992. Chemical isolation of quartz for measurement of in situ produced cosmogenic nuclides. Geochimica et Cosmochimica Acta 56, 3583–3587
- [31] Corbett, L. B., Bierman, P. R., & Rood, D. H. (2016). An approach for optimizing in situ cosmogenic 10Be sample preparation. *Quaternary Geochronology*, *33*, 24-34.

- [32] Corbett, L. B., Bierman, P. R., Woodruff, T. E., & Caffee, M. W. (2019). A homogeneous liquid reference material for monitoring the quality and reproducibility of in situ cosmogenic 10Be and 26Al analyses. *Nuclear Instruments and Methods in Physics Research Section B: Beam Interactions with Materials and Atoms*, 456, 180-185.
- [33] Rood, D. H., Hall, S., Guilderson, T. P., Finkel, R. C., & Brown, T. A. (2010). Challenges and opportunities in high-precision Be-10 measurements at CAMS. *Nuclear Instruments and Methods in Physics Research Section B: Beam Interactions with Materials and Atoms*, 268(7-8), 730-732.
- [34] Nishiizumi, K. (2004). Preparation of 26Al AMS standards. *Nuclear Instruments and Methods in Physics Research Section B: Beam Interactions with Materials and Atoms*, 223, 388-392.
- [35] Ramdohr, P. (1940). Eine Fundstelle von Beryllium-Mineralien im Gebiet der Kleinen Spitzkopje, Südwestafrika, und ihre Paragenese. *Neues Jahrbuch für Mineralogie, Geologie, und Palaöntologie*, 76, 1-35.
- [36] Merchel, S., Braucher, R., Lachner, J., & Rugel, G. (2021). Which is the best 9Be carrier for 10Be/9Be accelerator mass spectrometry? *MethodsX*, 8, 101486.
- [37] Makhubela, T. V., Kramers, J. D., Konyana, S. M., van Niekerk, H. S., & Winkler, S. R. (2021). Erosion rates and weathering timescales in the eastern Great Escarpment, South Africa. *Chemical Geology*, 580, 120368.

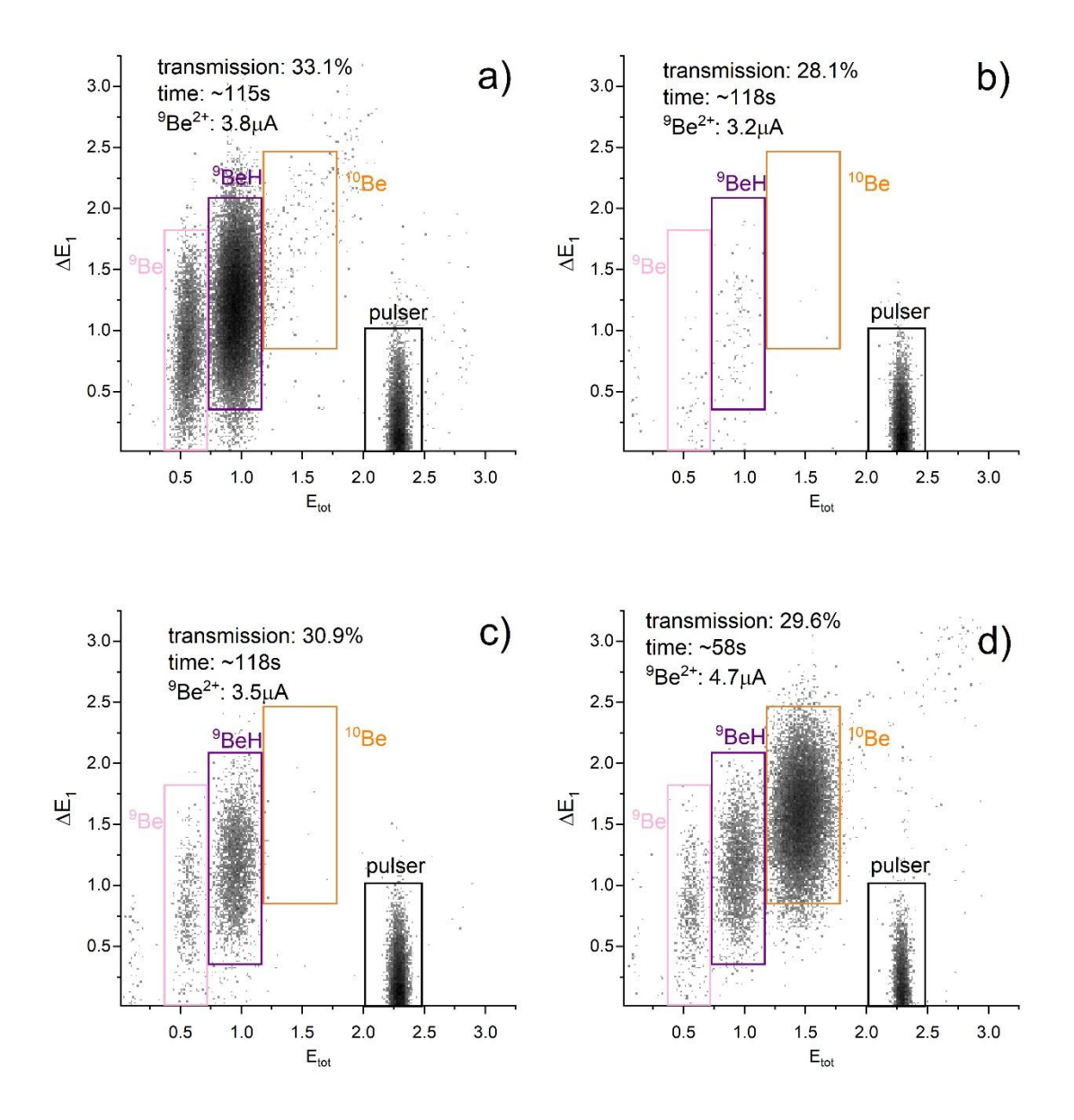


Schematic drawing of the iThemba LABS AMS systems. Symbols marking a type of component are labelled at least once. Orange components are electrostatic, blue components are magnetic for steering and focusing. Black is for electrostatic acceleration/deceleration. The drawing is not representative of relative scale.

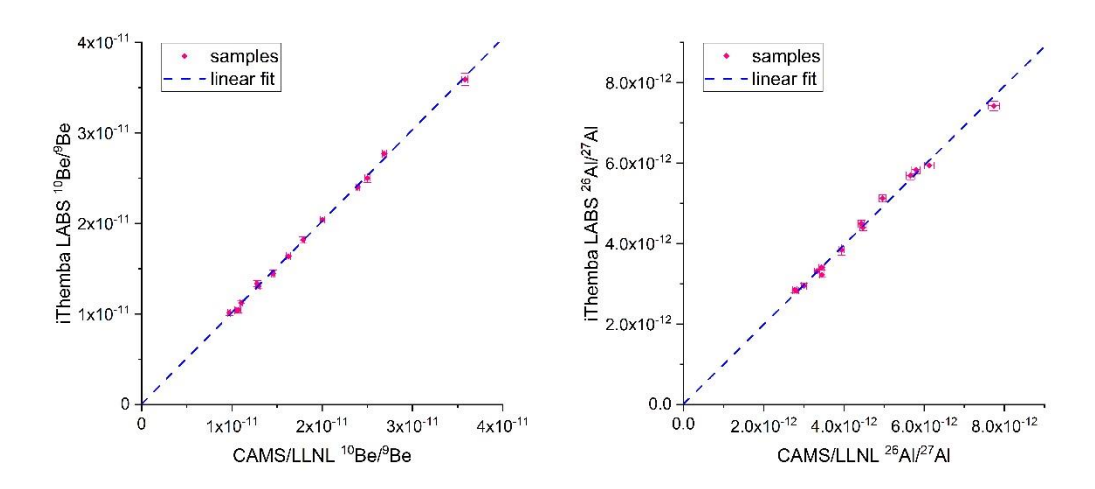
Figure 2



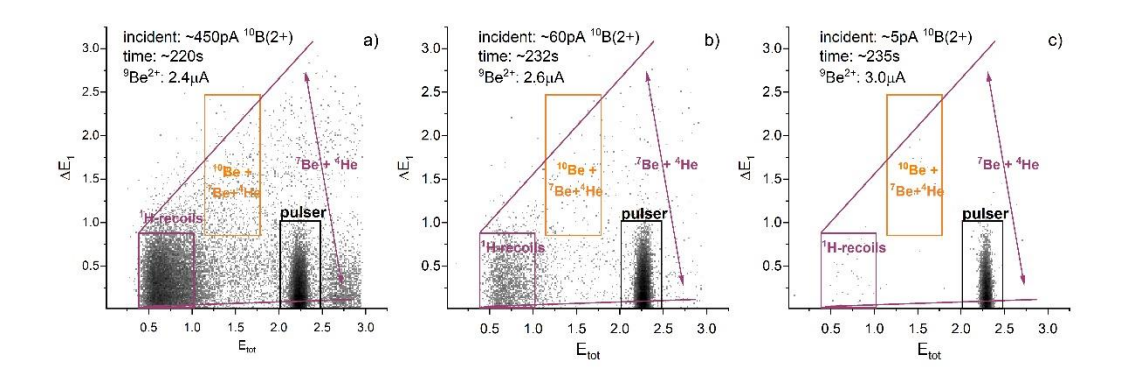
Foil stack thickness versus ¹⁰B residual energy. The boron beam was attenuated, and different gain settings were used for the individual spectra.



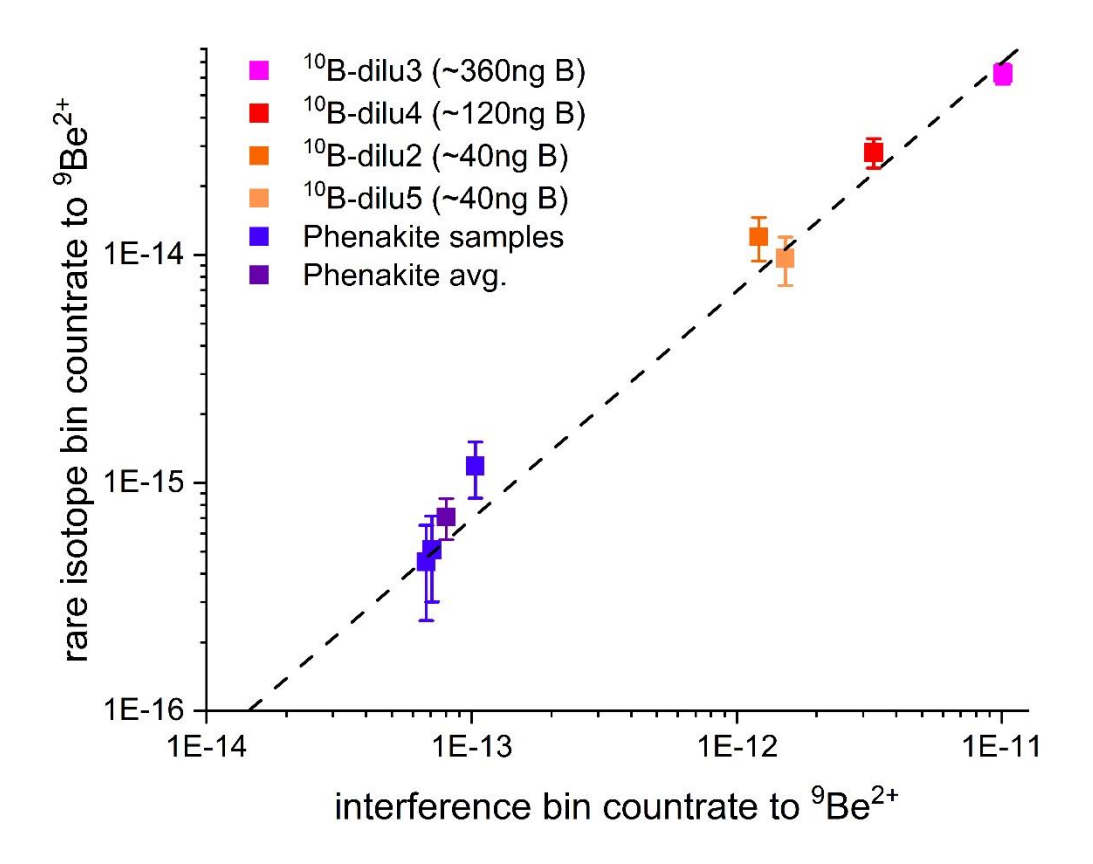
Spectra of E_{tot} versus ΔE_1 . Top row shows spectra for machine blanks at medium (a) and high stripper gas settings (b). Bottom row shows blank (Sigma Aldrich Beryllium Oxide) (c) and standard (KNSTD 01-5-1) (d). Identifiable signals are from $^{10}Be^{2+}$, $^9BeH^{2+}$ (with both 9Be and H arriving in the active detector volume), and 9Be with lost hydrogen.



Comparison of 14 field samples, as determined by iThemba LABS and CAMS/LLNL. The results are the blank corrected results given by each laboratory. The fitted linear for 10 Be has a slope of 1.010 ± 0.018 and an offset of $(0.5\pm3.1)\cdot10^{-13}$, consistent with zero. The Pearson's r is 0.9993.



Dilution series and nuclear reaction background dependent on the incident boron current. The final spectra (c) is from a phenakite Be-carrier sample without added boron. The background from nuclear reactions is present over the whole area between the solid purple lines, the spread indicated by the double arrow. The difficulty resolving the background better lies in the insufficient signal to noise ratio for the detector signals.



Detection limit and boron dilution series. The dashed line represents the boron-induced background counts in the rare isotope bin versus the main boron-induced background bin as ratio to ${}^9\mathrm{Be^{2^+}}$. This line can be used for background subtraction in the rare isotope bin. The phenakite samples fall on that line (within error) and thus are indistinguishable from our current measurement background.

Table 1

The first ¹⁰Be Kuni-standards series [114] at iThemba LABS in comparison. The ¹⁰Be/⁹Be of the commercial BeO (Alfa Aesar) material used as "blank" is not established.

Material	normalized to 5-1	uncertainty	nominal	ratio to nominal
KNSTD_5-1	2.709·10 ⁻¹¹	$2.2 \cdot 10^{-13}$	2.709·10 ⁻¹¹	1.000
KNSTD_5-4	2.854·10 ⁻¹²	8.6.10-14	2.851.10-12	1.001
KNSTD_6-2	5.510·10 ⁻¹³	3.3·10 ⁻¹⁴	5.350·10 ⁻¹³	1.030
BeO (Alfa Aesar)	3.0.10-14	1.2·10 ⁻¹⁴	-	-

Supplementary Figure 1

